Impaired Expression of *BCAT1* Relates to Muscle Atrophy of Mouse Model of Sarcopenia

Hui Ouyang
Peking University People's Hospital
Xuguang Gao
Peking University People's Hospital
Jun Zhang (happyluckyfish@163.com)
Peking University People's Hospital, Department of Neuromedicine, 11 Xizhimen South Street, Beijing, China;

Research

Keywords: sarcopenia, BCAT1, mTORC1, muscle, muscle atrophy

Posted Date: December 17th, 2020

DOI: https://doi.org/10.21203/rs.3.rs-127460/v1

Abstract

Background

The underlying mechanism of muscle atrophy in sarcopenia is still not fully understood; *BCAT1* isocitrate dehydrogenase-1 encodes an evolutionarily conserved cytoplasmic aminotransferase for glutamate and branched-chain amino acids (BCAAs), thus constituting a regulatory component of cytoplasmic amino and keto acid metabolism. In human gliomas carrying wild-type isocitrate dehydrogenase-1, BCAT1 promotes cell proliferation through amino acid catabolism. Hence, the goals of this study were to unravel the potential role of *BCAT1* expression in muscle atrophy and to explore the mechanisms underlying this process.

Methods

We first measured *BCAT1* expression by RT-qPCR and western blotting in murine and cellular models of muscle atrophy. To understand how the *BCAT1*-driven changes sustained muscle cell growth, we analyzed ROS levels and activation of the mTORC1/S6K1 pathway in muscle cells. Furthermore, we performed CCK8 assays and fluorescence staining to evaluate growth rate of cells and ROS levels. Finally, we verified that depletion of *BCAT1* impairs the growth rate of muscle cells and increases ROS levels, indicating that muscle atrophy resulted from the downregulation of the mTORC1/S6K1 pathway. Data were analyzed by two-tailed unpaired Student's *t*-test or Mann-Whitney U test for two groups to determine statistical significance. Statistical analyses were performed using GraphPad Prism version 6.0 and SPSS 16.0 software.

Results

BCAT1 expression level in skeletal muscles was lower in murine and cellular models of sarcopenia than in the control groups. *BCAT1* knockdown not only suppressed the growth of muscle cells but also increased the production of ROS. Impaired cell growth and increased ROS production was rescued by co-introduction of an shRNA-resistant *BCAT1* cDNA or addition of the mTORC1 stimulator MYH1485. Muscle cells with *BCAT1* knockdown featured lower mTORC1 and S6K1 phosphorylation (pS6K1) than NT muscle cells. Addition of either shRNA-resistant *BCAT1* cDNA or MYH1485 rescued the suppression of cell growth, increase in ROS production, and decrease in pS6K1.

Conclusions

The BCAA catabolic enzyme BCAT1 is essential for the growth of muscle cells. *BCAT1* expression contributes to sustained growth of muscle cells by activating mTOR signaling and reducing ROS production.

Introduction

Sarcopenia, the loss of skeletal muscle mass and function, is a debilitating consequence of cachexia, neuromuscular diseases, and diseases related to nerve injury. This loss of muscle function reduces the ability to recover from exercise. Therefore, patients with sarcopenia are at increased risk of physical weakness and death.

The etiologies of sarcopenia include aging, drug abuse, lack of activity, disease, and malnutrition, among others, many of which often coexist. However, the underlying mechanisms of muscle atrophy in sarcopenia are not fully understood [1].

Branched-chain amino acids (BCAAs) are essential amino acids that play an important regulatory role in nutrient signaling, body nitrogen metabolism, and protein synthesis [2]. The first enzymatic step is the reversible transamination catalyzed by branched chain amino acid transaminase (BCAT) isozymes (mitochondrial BCATm and cytosolic BCATc) [3]. The second step is the oxidative decarboxylation of branched-chain α-keto acids (BCKAs) to their respective branched chain acyl-CoA derivatives, which is coupled with the formation of NADH [4].

BCAT1 is an enzyme that initiates the catabolism of BCAAs. BCAT1 encodes an evolutionarily conserved cytoplasmic transaminase that acts on glutamate and BCAAs and thus constitutes a regulatory component of cytoplasmic amino and keto acid metabolism. BCAT1 promotes cell proliferation through amino acid catabolism in human gliomas carrying wild-type isocitrate dehydrogenase-1 [5]. Although skeletal muscle represents the most important site for BCAA transamination, the role of BCAT1 in human sarcopenia remains unknown. Low expression levels of BCATm and BCKDC were found to be associated with elevated plasma BCAAs [6], which may affect the mammalian (or mechanical) target of rapamycin (mTOR) pathway, more specifically, mTORC1, in peripheral tissues and influence protein synthesis [7].

Moreover, mTOR is a conserved serine/threonine kinase that plays a key role in cell growth and metabolism [8; 9]. The typical characteristic of mTOR activity is the decrease in phosphorylation of the downstream substrate S6K1 (pS6K1). Activation of the mTOR pathway (through mTORC1) can stimulate protein synthesis [10]. Furthermore, mTOR activity regulates protein synthesis by integrating and transforming various extracellular cues from growth factors and nutrients, as well as those related to cellular energy status and environmental pressure [11]. Among the two different intracellular mTOR complexes (mTORC1 and mTORC2), mTORC1 contains regulatory proteins related to mTOR, and is sensitive to rapamycin. Reportedly, mTORC1 is the most important regulator of protein synthesis [12], as it phosphorylates its downstream effectors S6K1 and 4E-BP in a rapamycin-sensitive manner [13; 14]. Additionally, mTORC1 regulates protein translation, cell proliferation, apoptosis, and autophagy. The mTORC1/S6K1 axis transmits and integrates important signals that are essential for biological processes involving nutrients, growth factors, and energy metabolites.

Previous studies have shown that mTORC1 activation was associated with muscle hypertrophy [15]. In addition, muscle-specific *raptor* gene knockout mice showed severe muscle atrophy and weight loss, leading to early death [16].

Therefore, the aims of this study were to investigate the potential role of *BCAT1* expression in muscle atrophy, and to further explore the underlying mechanism. We first measured the expression of *BCAT1* in murine and cellular models of muscle atrophy. To understand how *BCAT1*-driven changes affected muscle cell growth, we analyzed reactive oxygen species (ROS) levels in muscle cells and activation of the mTORC1/S6K1 pathway. Finally, we validated our hypothesis that *BCAT1* depletion could induce muscle atrophy by downregulating the mTORC1/S6K1 pathway and increasing ROS levels.

Materials And Methods

Mice

Male C57BL/6 mice were divided into two groups (n = 5-7): control and dexamethasone (DEX)-induced sarcopenia groups. The mice were obtained from the Health Science Center of Peking University. In this study, the average age of the animals was 10 weeks. Fresh muscle samples were stored at –80 °C. All animal experiments were approved by the Animal Care and Use Committee of Peking University People's Hospital.

Generation of a mouse model of sarcopenia

The control group was intraperitoneally injected with sterile normal saline over 10 days, and the sarcopenia group was intraperitoneally injected with 25 mg/kg/day of water-soluble DEX (Sigma Aldrich) for 10 days [17]. The animals were euthanized on day 11. Body weights were measured, and total muscle mass, tibial anterior muscles, and gastrocnemius muscles were removed, weighed, and quickly frozen for analysis of mRNA and protein levels.

2.3 Cell culture

Murine C2C12 myoblasts were cultured as recommended by the supplier (Cell Resource Bank of the Chinese Academy of Sciences). In short, C2C12 myoblasts were maintained in DMEM supplemented with 10% FBS, 100 U/mL penicillin, and 100 U/mL streptomycin. For routine differentiation, the cells were grown to approximately 80% confluence.

2.4 Immunofluorescence staining

C2C12 cells were cultured in multiwells, treated with DEX (1 μM) or sterile saline for 24 h, fixed with 4% paraformaldehyde at 4 °C, washed three times with phosphate-buffered saline (PBS), permeabilized with 0.3% Triton X-100, washed three times with PBS, blocked with 10% goat serum in PBS, and incubated with primary antibody diluted in PBS (1:200) at 4 °C. After three sequential washes with PBS, the cells were incubated with fluorescently labeled donkey anti-rabbit IgG (H+L) as secondary antibody (594) diluted in PBS (1:300) at 4 °C, and washed three times with PBS afterwards. The nuclei were counterstained with DAPI and subsequently washed with PBS. Digital images of fluorescently labeled cells were obtained using a fluorescence microscope (Olympus IX51, Japan).

2.5 SDS-PAGE and western blot analysis

The cell samples were directly dissolved in cryolysis buffer [RIPA buffer (Beyotime, China), PMSF (Amresco, China), cocktail (Shanghai Yuanye, China), Triton X-100 (China Amresco), and NaVO3] for 15 min. The lysates were clarified by centrifugation (12,000 × *g,* 15 min at 4 °C). The supernatant was collected and stored at –80 °C. Protein concentration was determined using the Beyond Time™ BCA Test Kit (Shanghai Beiotim Biotechnology Company, China). For western blotting, SDS-PAGE was used to separate the same amount of protein per sample, which was then transferred to a PVDF membrane (Millipore, USA). Afterwards, the membrane was incubated with 5% skimmed milk in Tris-buffered saline with Tween20 (TBS-T buffer) for 2 h, followed by addition of the primary antibodies against the indicator proteins at 4 °C. Then, the appropriate horseradish peroxidase-coupled secondary antibody was added, and the membrane was washed with TBS-T at room temperature for 2 h. Immune response bands were detected by an enhanced chemiluminescence system and analyzed by Quantity One software (Pierce ECL, western blotting substrate; Thermo Fisher Scientific, Pierce, Rockford, IL, US). ImageJ software [18] was used to quantify each protein band and standardize it to a loading control (GAPDH).

2.6 Cell viability analysis

Cell viability was determined by the CCK8 assay according to the manufacturer's instructions (China). Cells were used at a density of 2×10^3 cells/well. After treatment with DEX or sterile normal saline, the monolayer was washed three times with PBS, and 10 μL of CCK8 reagent-containing DMEM solution was added and incubated at 37 °C for 2 h. Absorbance was measured using a microplate reader at 450 nm and expressed as percentage of the control value.

2.7 Viral constructs and virus production

Full-length cDNA of mouse *BCAT1* (MAGE clone ID 30063465) was cloned into the plvx-puro-3xlag vector. Plvx-puro-3xlag and plko.1-puro-gfp vectors were obtained from Geneline Bioscience. Short hairpin RNA (shRNA) directed against *BCAT1* mRNA (shBCAT1) was designed and cloned on the plko.1-puro-gfp vector. Target and control sequences were 5'-ccggcccagcatagtatttcgaataccttgtgtttttttggttg-3' and 5'-ccggcccagagaggcggctacttagttg-3', respectively. Interference of the product generated by employing the primers BCAT1-f (5'-ctcatcacacagcca-3') and BCAT1-r (5'-ctatccatgtggtcgg-3') with *BCAT1* expression was verified by PCR. HEK293T cells were transfected with polybrenylamine and Hg transgenic reagent (China) for virus production. The virus-containing supernatant was collected for 48 h and then concentrated by ultracentrifugation at 4,500 × *g* for 35 min.

2.8 ROS production

ROS production was measured by using a Cellular Reactive Oxygen Species Detection Assay (Abcam, England). Cells were seeded on 20-well plates and incubated with 5 μM dichlorodihydrofluorescein diacetate (DCFH-DA) for 20-30 min and subsequently washed twice with PBS. Changes in relative fluorescence were measured using a fluorescence microscope (Olympus IX51, Japan).

2.9 RNA isolation and quantitative real-time PCR (RT-qPCR)

The gastrocnemius muscle was homogenized in Trizol reagent (Transgen Biotechnology, Beijing, China) on ice, and then separated into organic and aqueous phases by chloroform. After ethanol precipitation, total RNA was extracted from the aqueous phase. RT-qPCR was performed by Transgen Biotechnology (Beijing). *BCAT1* expression was quantified using the thermal cycling dice real-time system and SYBR premix ex Taq II (Takara Bio, Shiga, Japan). All samples were measured in duplicate. GAPDH was used as an internal control to evaluate any variation due to reverse transcription and PCR efficiencies. There was no change in expression between the different groups analyzed. The forward and reverse primers used for detection of these genes were as follows: mus GAPDH-F: 5′-cgagatgggaagttgtca-3′, GAPDH-R: 5′-cgagatggaagcttgtca-3′; mus BCAT1-F: 5′-ctcatcatcacacaccaccagca-3′, and BCAT1-R: 5′-ctatccatgtggtcgg-3′.

2.10 Whole muscle lysates

The gastrocnemius muscle was homogenized in RIPA buffer (25 mM Tris-HCl, pH 7.6, 150 mM NaCl, 1% NP-40, 1% sodium deoxycholate, and 0.1% SDS) supplemented with a mixture of protease and phosphatase inhibitors (Thermo Fisher Scientific, US). The whole procedure was performed on ice.

2.11 Preparation of frozen sections

Fresh gastrocnemius muscles were dissected, frozen in n-hexane at –70 °C, and cooled in liquid nitrogen for 2 min. Cross sections (10 μm) were cut at –20 °C using a cryostat slicer and stained with nicotinamide adenine dinucleotide hydrogen (NADH) according to a previously described method [19].

2.12 Antibodies

Polyclonal anti-BCAT1 antibody (13640-1-ap; Protein Tech) was used for immunofluorescence staining. Western blotting was performed using the following antibodies: rabbit polyclonal anti-BCAT1 (13640-1-ap), anti-pS6K1 (ab59208; Abcam), rabbit monoclonal anti-p-mTOR (ab109268; Abcam), anti-mTOR (ab32028; Abcam), anti-S6K1 (ab32359; Abcam), and mouse monoclonal anti-GAPDH (60004-1-lg; Protein Tech).

2.13 Statistical analysis

Data were analyzed using Student's *t*-test or Mann Whitney U test. Unless specified otherwise, values are presented as mean ± standard deviation, and $p < 0.05$ was considered statistically significant. Statistical analyses were performed using GraphPad Prism 6.0 or SPSS 16.0 software.

2.14 Data availability

All other relevant data are available from the corresponding author upon request.

Results

3.1 Skeletal muscle mass, muscle atrophy, and *BCAT1* expression

Animal characteristics are shown in Table 1. The average body weight of DEX-induced sarcopenia mice was lower than that of the mice in the control group. Absolute and total masses of the gastrocnemius and tibialis anterior muscles were measured, and the sarcopenic index was calculated. The absolute muscle mass and sarcopenia index in the sarcopenic group were lower than those in the control group. Compared with the control group, muscle atrophy was more pronounced in the sarcopenia group (Fig. 1B-C).

To investigate the role of BCAT1 in DEX-induced muscle atrophy in mice, we measured *BCAT1* expression level in skeletal muscles (gastrocnemius and tibialis anterior muscles) of mice, and found that *BCAT1* expression in skeletal muscle in the sarcopenic group was lower than that in the control group (Fig. 1A).

3.2 *BCAT1* expression is downregulated in DEX-treated muscle cells

To investigate the role of BCAT1 in muscle atrophy, C2C12 cells were treated with DEX to establish a cellular model of muscle atrophy. We confirmed that C2C12 cell growth was impaired upon DEX treatment (Fig. 2D). Next, we investigated *BCAT1* expression in C2C12 cells. BCAT1 protein expression in growth-restricted C2C12 cells was lower than that in normal muscle cells (Fig. 2A-C). Thus, growth-impaired muscle cells featured reduced *BCAT1* expression, suggesting the potential role of BCAT1 in growth retardation and atrophy of myocytes.

3.3 *BCAT1* knockdown impairs growth and promotes ROS production in C2C12 cells

Since *BCAT1* expression was downregulated in a DEX-induced cellular muscle atrophy model, we wanted to determine the role of BCAT1 in the pathogenesis of muscle atrophy. Therefore, we prepared lentivirus, which could knock down the expression of BCAT1, the first enzyme in the BCAA catabolic pathway, in C2C12 muscle cells. *BCAT1* knockdown inhibited the growth rate of C2C12 cells from day 2 (Fig. 3A). Next, we studied the mechanisms by which BCAT1 contributed to muscle cell growth. Therefore, we analyzed whether loss of BCAT1 increased ROS production. Compared with the vector control group, shBCAT1 (*BCAT1* gene knockdown) inhibited the growth of muscle cells *in vitro*. Further evidence suggested that *BCAT1* knockdown not only inhibited the growth of the muscle cells but also increased the production of ROS (Fig. 3B), which in turn inhibited cell growth. Quantitative analysis of cell viability according to the CCK8 assay showed that cell growth in the *BCAT1* knockdown group was decreased after 24 h, which was not statistically significant. After 48 h, quantitative data showed that cell growth had decreased significantly in response to *BCAT1* knockdown compared with the control group (Fig. 3A). *BCAT1* knockdown also significantly promoted ROS production (Fig. 3B). Combined introduction of anti-shRNA *BCAT1* cDNA or the mTORC1 stimulator MYH1485 alleviated both impaired cell growth and increased ROS production (Fig. 3A-B). In conclusion, these findings suggest that BCAT1 contributes to the maintenance of muscle cell growth and limits ROS production.

3.4 mTOR contributes to BCAT1 function in muscle cells

Finally, we asked how the metabolic regulator BCAT1 affected muscle cell growth and ROS production. To understand this, we analyzed ROS levels and activation of the mTORC1/S6K1 pathway in myocytes. Western blotting was used to determine the phosphorylation status and total protein concentration of the mTORC1 downstream target S6K1 in the gastrocnemius muscle. As shown in Fig. 4, the ratios of p-mTOR and mTOR, as well as those of pS6K1 and S6K1 in the *BCAT1* knockdown group were significantly reduced compared with the control group. These results suggested that *BCAT1* knockdown inhibited the activation of mTOR and S6K1 downstream of the mTORC1 kinase. To further confirm the role of the mTOR1/S6K1 axis in *BCAT1* knockdown-induced muscle cell growth impairment, we used shRNA-resistant *BCAT1* cDNA and mTOR activators/inhibitors. Compared with the shBCAT1 plasmid, the viability of muscle cells transfected with anti-BCAT1 shRNA could be recovered significantly. In addition, myocytes treated with the mTOR activator MYH1485 showed improved cell viability, while muscle cells treated with an mTOR inhibitor were damaged. Treatment with MYH1485, an activator of mTOR, was associated with significantly reduced cell viability after shBCAT1 transfection. Rapamycin, an mTOR inhibitor, blocked the effect of BCAT1 on cell viability and growth. In conclusion, compared with NT myocytes, the phosphorylation levels of mTORC1 and S6K1 in growth-impaired myocytes were lower, which indicated that decreased *BCAT1* expression in muscle cells resulted in the weakening of mTORC1-dependent signal transduction. Anti-shRNA-BCAT1 cDNA and the mTORC1 stimulator MYH1485 were able to restore cell growth, ROS production, and pS6K1 levels. These results suggest that BCAT1 may maintain myocyte growth and limit ROS production through the mTORC1/S6K1 axis.

Discussion

Although *BCAT1* is mainly expressed in skeletal muscle and plays an important role in muscle energy metabolism, the molecular basis of its involvement in the pathogenesis of muscle atrophy is still unclear.

In this study, we put forward some important suggestions. First, we found that *BCAT1* expression was downregulated in a model of muscle atrophy. Second, we demonstrated for the first time that BCAT1 could maintain muscle cell growth and reduce ROS production. Third, we found that BCAT1 regulated muscle cell growth and ROS production through the mTORC1/S6K1 signaling pathway. These results suggest that downregulation of BCAT1 and mTORC1/S6K1 pathway is one of the reasons for impaired cell growth in atrophic muscle cells.

BCAAs are the cornerstone of protein synthesis and energy provision [20]. However, the relative importance of the bioenergy contribution of amino acids in muscle is still unclear under both physiological and pathological conditions. BCAT1 is the first enzyme to initiate the catabolism of BCAAs. Our study provides additional evidence that downregulation of BCAT1 had adverse effects on muscle cell growth and ROS production.

Accumulating evidence suggests that regulation of mTOR is essential for cell growth. Cardiomyocyte-specific mTOR depletion led to decreased proliferation and increased apoptosis, resulting in a decrease in

embryonic heart size [21]. However, whether BCAT1 affected the regulation of mTOR1/S6K1 signal transduction remained unclear. This study provides an insight into the roles of the BCAT1/mTOR/S6K1 pathway. Our results indicate for the first time that BCAT1 depletion significantly reduced the activation of the mTORC1/S6K1 signaling pathway in muscle cells. Therefore, we established a link between BCAT1 and muscular atrophy/sarcopenia.

BCAT1 increases the mitochondrial content by activating key regulatory factors of mitochondrial biogenesis [21]. Our results suggest that BCAT1 may promote mitochondrial function and cell growth by reducing ROS production and regulating a variety of nutritional sensors, including mTOR and S6K1. Interestingly, we found that BCAT1 could activate mTOR signaling and downregulate ROS production. Rapamycin inhibited mTOR signaling and blocked the effect of BCAT1 on ROS production and subsequent cell growth impairment. Because BCAT1 depletion decreased the levels of p-mTOR and pS6K1, *BCAT1* expression is presumed to positively regulate mTORC1 activation. Importantly, shRNA-resistant *BCAT1* cDNA and mTOR activators effectively reversed the growth impairment induced by *BCAT1* knockdown and led to increased pS6K1 levels in a rapamycin-sensitive manner. In conclusion, we assigned an important role to the BCAT1/mTOR axis with regard to the pathogenesis of muscle atrophy, and provide theoretical proof for reducing muscle atrophy by regulating the BCAT1/mTOR pathway. However, further studies are needed to explain how the catabolic enzyme BCAT1 activates mTOR in muscle cells.

In conclusion, we demonstrated that BCAT1 is essential for the growth of muscle cells. BCAT1 maintains muscle cell growth by activating mTOR signaling and reducing ROS production. Therefore, stable *BCAT1* expression is necessary to maintain the growth of muscle cells and reduce ROS production. Moreover, BCAT1 may be a potential target for the treatment of muscle atrophy. Our observations highlight potential therapeutic targets for nutritional or pharmaceutical interventions aimed at reducing severe weight loss in patients with muscular atrophy.

In view of the limitations faced in the current study, we have no evidence that BCAT1 regulates the mTORC1/S6K1 signaling pathway *in vivo*. Moreover, we have not explored other important factors or molecules related to muscle atrophy, such as inflammation and Notch signaling, among others. To to compensate for this, we plan to use the *BCAT1* knockdown animal model to verify our findings and explore other effects and mechanisms of BCAT1 in muscle atrophy. Accordingly, further experiments are needed to confirm whether BCAT1 is also involved in the development of muscle atrophy *in vivo*, and whether changes in BCAT1 levels are associated with the progression of muscle atrophy.

Abbreviations

BCAAs branched-chain amino acids

BCKAs branched-chain keto acids

BCAT1 branched-chain aminotransferase 1

WT wild-type

mTOR mammalian target of rapamycin

mTORC1 complex 1 of mTOR pathway

α-KG α-ketoglutarate

S6K1 70-kDa ribosomal protein S6 kinase 1

Declarations

Acknowledgments

We thank Prof. Weidong Yu, Dr Daojun Hong and Dr Yang He for their helpful advices, we thank Ling Liu for technical assistance.

Funding

This work was supported by the National Science Foundation of China (No.81870996).

Availability of data and materials

Not applicable

Authors' contributions

Hui Ouyang and Jun Zhang performed the experiments. Hui Ouyang and Xuguang Gao designed and analyzed all studies. The manuscript was written by Hui Ouyang and edited by Jun Zhang and Xuguang Gao. All authors read and approved the final manuscript.

Ethics approval and consent to participate

All of animal experimental procedures were approved by the Ethical Committee of Peking University People's Hospital, China.

Consent for publication

Not applicable

Competing interests

The authors declare that they have no competing interests.

References

[1] F. Riuzzi, and G. Sorci, Cellular and molecular mechanisms of sarcopenia: the S100B perspective. (2018).

[2] M.G. Vander Heiden, Targeting cancer metabolism: a therapeutic window opens. Nature reviews. Drug discovery 10 (2011) 671-84.

[3] M. Bixel, Y. Shimomura, S. Hutson, and B. Hamprecht, Distribution of key enzymes of branched-chain amino acid metabolism in glial and neuronal cells in culture. The journal of histochemistry and cytochemistry : official journal of the Histochemistry Society 49 (2001) 407-18.

[4] A.J. Sweatt, M. Wood, A. Suryawan, R. Wallin, M.C. Willingham, and S.M. Hutson, Branched-chain amino acid catabolism: unique segregation of pathway enzymes in organ systems and peripheral nerves. American journal of physiology. Endocrinology and metabolism 286 (2004) E64-76.

[5] M. Tönjes, S. Barbus, Y.J. Park, W. Wang, M. Schlotter, A.M. Lindroth, S.V. Pleier, A.H.C. Bai, D. Karra, R.M. Piro, J. Felsberg, A. Addington, D. Lemke, I. Weibrecht, V. Hovestadt, C.G. Rolli, B. Campos, S. Turcan, D. Sturm, H. Witt, T.A. Chan, C. Herold-Mende, R. Kemkemer, R. König, K. Schmidt, W.E. Hull, S.M. Pfister, M. Jugold, S.M. Hutson, C. Plass, J.G. Okun, G. Reifenberger, P. Lichter, and B. Radlwimmer, BCAT1 promotes cell proliferation through amino acid catabolism in gliomas carrying wild-type IDH1. Nature medicine 19 (2013) 901-908.

[6] P. She, C. Van Horn, T. Reid, S.M. Hutson, R.N. Cooney, and C.J. Lynch, Obesity-related elevations in plasma leucine are associated with alterations in enzymes involved in branched-chain amino acid metabolism. American journal of physiology. Endocrinology and metabolism 293 (2007) E1552-63.

[7] C.J. Lynch, B.J. Patson, J. Anthony, A. Vaval, L.S. Jefferson, and T.C. Vary, Leucine is a direct-acting nutrient signal that regulates protein synthesis in adipose tissue. American journal of physiology. Endocrinology and metabolism 283 (2002) E503-13.

[8] V. Albert, and M.N. Hall, mTOR signaling in cellular and organismal energetics. Current opinion in cell biology 33 (2015) 55-66.

[9] M. Laplante, and D.M. Sabatini, mTOR signaling in growth control and disease. Cell 149 (2012) 274-93.

[10] S. Rentas, N. Holzapfel, M.S. Belew, G. Pratt, V. Voisin, B.T. Wilhelm, G.D. Bader, G.W. Yeo, and K.J. Hope, Musashi-2 attenuates AHR signalling to expand human haematopoietic stem cells. Nature 532 (2016) 508-511.

[11] E.A. Dunlop, and A.R. Tee, Mammalian target of rapamycin complex 1: signalling inputs, substrates and feedback mechanisms. Cellular signalling 21 (2009) 827-35.

[12] E. Jacinto, R. Loewith, A. Schmidt, S. Lin, M.A. Rüegg, A. Hall, and M.N. Hall, Mammalian TOR complex 2 controls the actin cytoskeleton and is rapamycin insensitive. Nature cell biology 6 (2004)

1122-8.

[13] G.Q. Daley, R.A. Van Etten, and D. Baltimore, Induction of chronic myelogenous leukemia in mice by the P210bcr/abl gene of the Philadelphia chromosome. Science (New York, N.Y.) 247 (1990) 824-30.

[14] T. Imai, A. Tokunaga, T. Yoshida, M. Hashimoto, K. Mikoshiba, G. Weinmaster, M. Nakafuku, and H. Okano, The neural RNA-binding protein Musashi1 translationally regulates mammalian numb gene expression by interacting with its mRNA. Molecular and cellular biology 21 (2001) 3888-900.

[15] S.C. Bodine, T.N. Stitt, M. Gonzalez, W.O. Kline, G.L. Stover, R. Bauerlein, E. Zlotchenko, A. Scrimgeour, J.C. Lawrence, D.J. Glass, and G.D. Yancopoulos, Akt/mTOR pathway is a crucial regulator of skeletal muscle hypertrophy and can prevent muscle atrophy in vivo. Nature cell biology 3 (2001) 1014-9.

[16] C.F. Bentzinger, K. Romanino, D. Cloëtta, S. Lin, J.B. Mascarenhas, F. Oliveri, J. Xia, E. Casanova, C.F. Costa, M. Brink, F. Zorzato, M.N. Hall, and M.A. Rüegg, Skeletal muscle-specific ablation of raptor, but not of rictor, causes metabolic changes and results in muscle dystrophy. Cell metabolism 8 (2008) 411-24.

[17] S.R. Jesinkey, M.C. Korrapati, K.A. Rasbach, C.C. Beeson, and R.G. Schnellmann, Atomoxetine prevents dexamethasone-induced skeletal muscle atrophy in mice. The Journal of pharmacology and experimental therapeutics 351 (2014) 663-73.

[18] X.F. Qin, D.S. An, I.S. Chen, and D. Baltimore, Inhibiting HIV-1 infection in human T cells by lentiviral-mediated delivery of small interfering RNA against CCR5. Proceedings of the National Academy of Sciences of the United States of America 100 (2003) 183-8.

[19] L. Song, Y. Gao, X. Zhang, and W. Le, Galactooligosaccharide improves the animal survival and alleviates motor neuron death in SOD1G93A mouse model of amyotrophic lateral sclerosis. Neuroscience 246 (2013) 281-90.

[20] H. Taegtmeyer, M.E. Harinstein, and M. Gheorghiade, More than bricks and mortar: comments on protein and amino acid metabolism in the heart. The American journal of cardiology 101 (2008) 3e-7e.

[21] M.A. Joshi, N.H. Jeoung, M. Obayashi, E.M. Hattab, E.G. Brocken, E.A. Liechty, M.J. Kubek, K.M. Vattem, R.C. Wek, and R.A. Harris, Impaired growth and neurological abnormalities in branched-chain alpha-keto acid dehydrogenase kinase-deficient mice. The Biochemical journal 400 (2006) 153-62.

Tables

Table 1. Weight of muscles from dexamethasone-induced atrophy in C57BL/6 mice.

	Control	DEX	**p** value
Tibialis anterior muscle	0.65 ± 0.03	0.46 ± 0.03	< 0.01*
Gastrocnemius muscle	1.27 ± 0.03	0.96 ± 0.08	< 0.01*
Total muscle mass	3.92 ± 0.13	2.85 ± 0.11	< 0.01*
Body weight	28.75 ± 0.54	21.72 ± 0.54	< 0.01*
Sarcopenia index	0.136 ± 0.003	0.131 ± 0.004	0.039*

Data are presented as mean ± SEM (n = 6); * p < 0.05 based on Student's *t*-test; DEX, dexamethasone

Figures

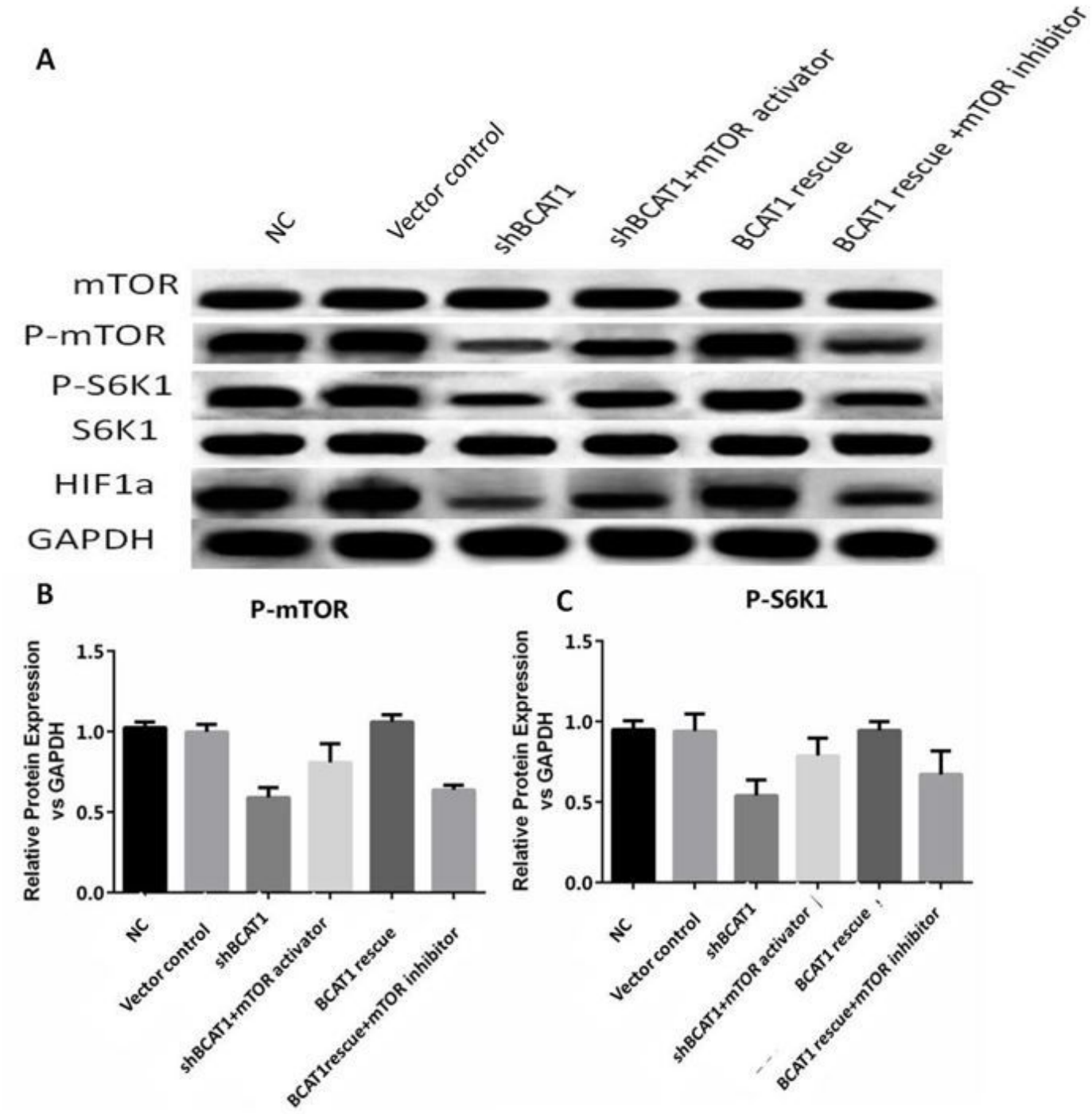

Figure 1

Inhibitory effect of BCAT1 knockdown on activation of the mTORC1-S6K1 signal pathway. (A) Immunoblot analysis of mTOR, p-mTOR, pS6K1, and S6K1 in mouse C2C12 cells. Grouping: control vector (shCtrl), shBCAT1, shBCAT1 + mTOR activator, shBCAT1 + shRNA-resistant BCAT1 cDNA (rescue), shBCAT1 + shRNA-resistant BCAT1 cDNA (rescue) + mTOR inhibitor, n = 3, cells were analyzed at 24 h post-treatment. Representative images of protein levels of mTOR, p-mTOR, S6K1, and pS6K1 in muscle cells are presented. (B-C) Quantitative analysis of protein levels of p-mTOR and pS6K1, where the relative

band intensity was normalized to GAPDH. Data from three independent experiments are presented as mean + SEM.

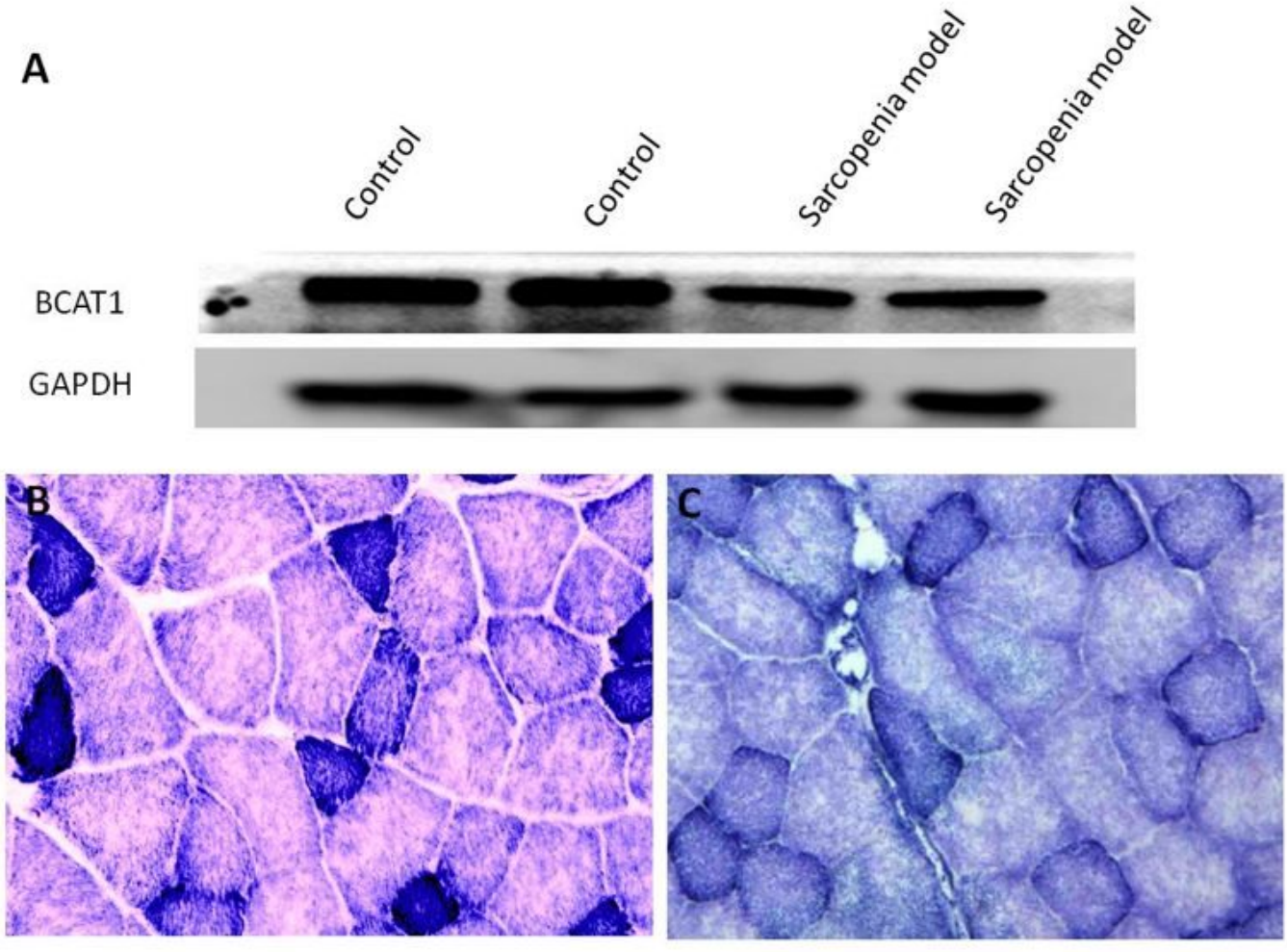

Figure 1

Dexamethasone (DEX) treatment induces muscle atrophy and impaired muscle BCAT1 expression in mice. (A) DEX-induced muscle atrophy is associated with reduced BCAT1 expression. BCAT1 protein expression was determined by western blotting using samples from the gastrocnemius muscle of control mice and mice with muscle atrophy. GAPDH was used as a loading control. (B) NADH staining of the gastrocnemius muscle of mice in the DEX-induced muscle atrophy group. (C) NADH staining of the gastrocnemius muscle of mice in the control group.

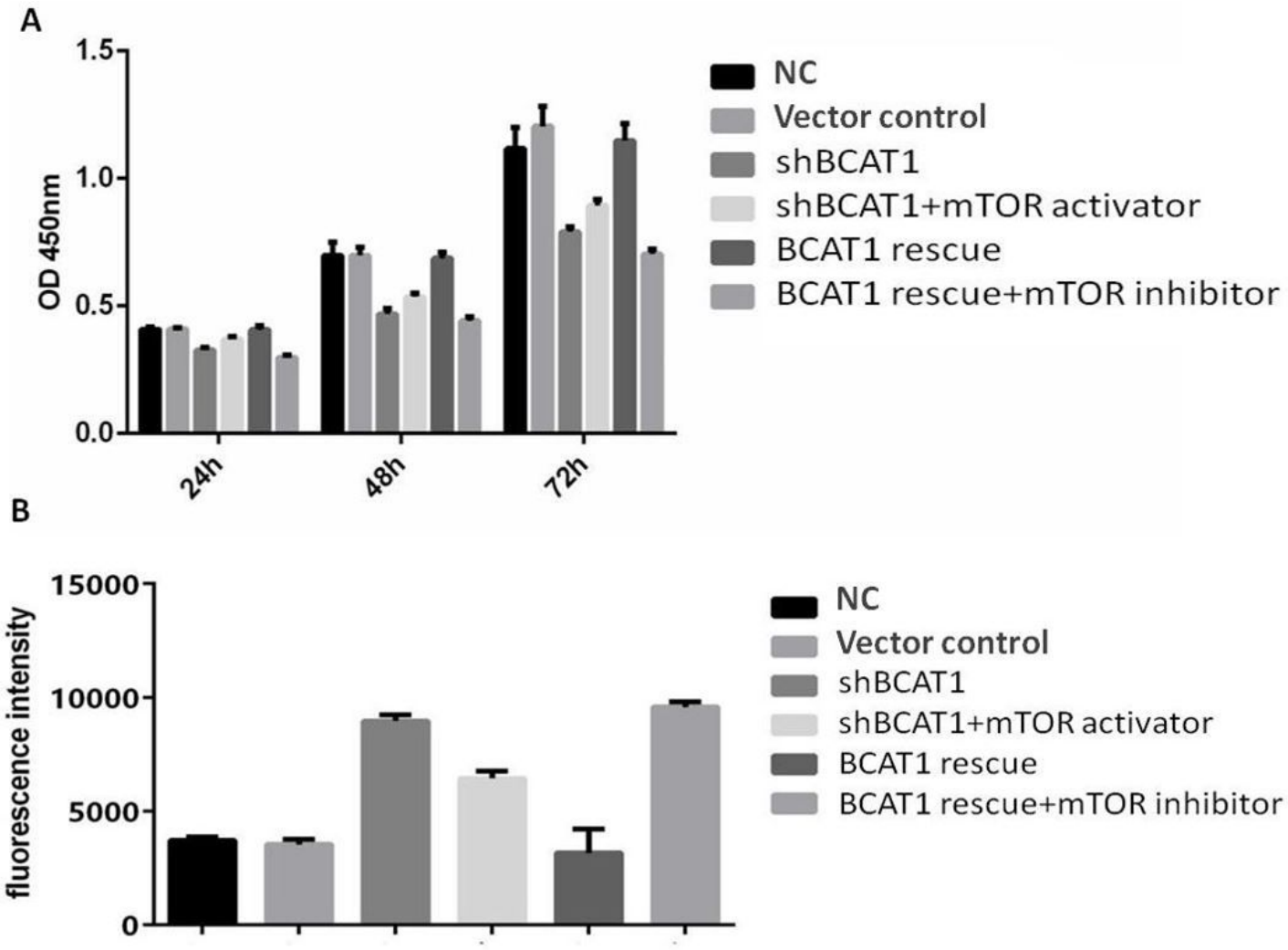

Figure 1

BCAT1 knockdown impairs cell growth and promotes ROS production in muscle cells. (A) Viability of C2C12 cells was detected by the CCK8 method. Grouping: control vector (shCtrl), shBCAT1, shBCAT1 + mTOR activator, shBCAT1 + shRNA-resistant BCAT1 cDNA (rescue), shBCAT1 + shRNA-resistant BCAT1 cDNA (rescue) + mTOR inhibitor, n = 3, cells were analyzed at 24 h post-treatment. (B) ROS concentration in C2C12 cells was detected by the fluorescence method. Grouping: control vector (shCtrl), shBCAT1, shBCAT1 + mTOR activator, shBCAT1 + shRNA-resistant BCAT1 cDNA (rescue), shBCAT1 + shRNA-resistant BCAT1 cDNA (rescue) + mTOR inhibitor, n = 3, cells were analyzed at 24 h post-treatment. Data from three independent experiments are presented as mean + SEM.

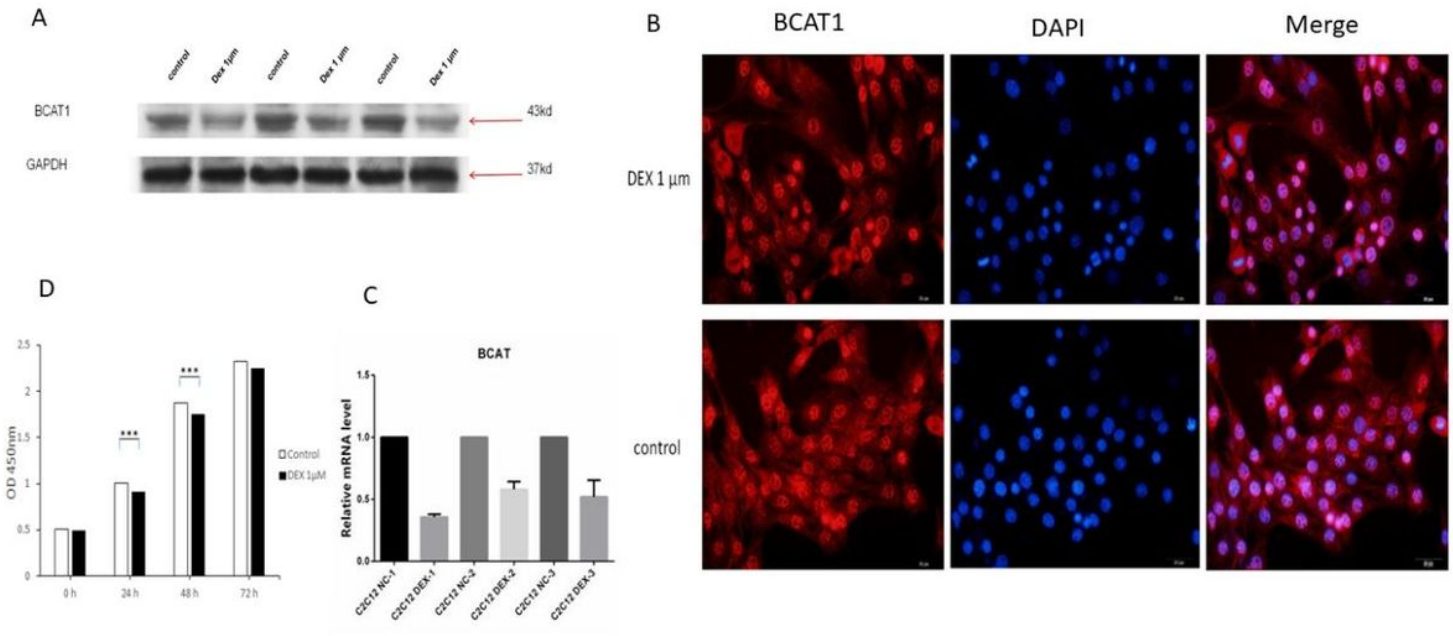

Figure 1

BCAT1 expression is downregulated in dexamethasone (DEX)-treated C2C12 cells. (A) Immunoblot analysis of BCAT1 protein levels in C2C12 cells cultured in presence and absence of DEX (1 μm, 24 h); n = 3 per group. (B) Immunofluorescence detection of BCAT1 in C2C12 muscle cells with or without DEX (1 μm, 24 h). Cellular localization of the proteins was subsequently determined using fluorescence microscopy following fixation and incubation with DAPI to label cell nuclei. The BCAT1-specific signal (green) indicates total BCAT1 expression, whereas DAPI counterstaining (blue) indicates the position of the nuclei; n = 3 per group. (C) BCAT1 mRNA expression in C2C12 cells with or without DEX treatment (1 μm, 24 h), where relative mRNA levels are representative of the mean value; n = 3 per group. (D) C2C12 cells were cultured in presence of absence of DEX (1 μm, 24 h), after which cell viability was determined by the CCK8 method. Data from three independent experiments are presented as mean + SEM; n = 3 per group